

****TITLE****
*ASP Conference Series, Vol. **VOLUME**, **PUBLICATION YEAR***
****EDITORS****

Chandra and RXTE Observations of X-ray Novae

Jeffrey E. McClintock

*Harvard-Smithsonian Center for Astrophysics, 60 Garden Street,
Cambridge, MA 02138, U.S.A.*

Abstract. We discuss new observations of X-ray novae with *Chandra* which provide strong evidence that black holes have event horizons. The evidence is based on the finding that black hole X-ray novae in quiescence are approximately 100 times fainter than equivalent neutron star X-ray novae. The advection-dominated accretion flow model provides a natural explanation for this difference. *RXTE* observations of XTE J1550-564 in the *very high* state, which were obtained during the 1998-1999 outburst of the source, reveal an extraordinarily tight correlation between the central frequency of the low frequency QPO and the soft, non-power-law flux in the 2-20 keV band. We discuss the nature of this soft spectral component and suggest the importance of obtaining direct observations of it at low energies ($E < 2$ keV) at the first available opportunity.

1. Memories of Jan

I collaborated on several papers with Jan in the 1970s and 1980s. In 1991 we began to work together on a review chapter for the book “X-ray Binaries.” Then suddenly my 17-year-old daughter was killed in an automobile accident. I was unable to work for many months. Finally, I became concerned about the schedule for the review chapter. Jan somehow convinced me not to worry at all – that I should return to work only when I felt ready. Meanwhile, he was under intense pressure, since he was writing one chapter himself, collaborating on yet another, and helping to edit the entire volume as well. Eventually we finished our chapter, and during the whole time he never pressured me at all. I am extremely grateful for his compassion and support.

On another occasion, I experienced a different aspect of Jan’s character. A collaborator and I had referred to some work of Jan’s in a sloppy way, without giving him and his students proper credit. Jan immediately sent us a bristling email that read: “We already said that! We’re not just fooling around here!” In this case, Jan was being honest, direct and effective. I learned a lot more than astrophysics from Jan.

My talk is in three parts. First, I briefly describe black hole X-ray novae and neutron star X-ray novae. Second, I summarize the evidence that the black hole primaries in X-ray novae possess event horizons. Finally, I discuss the spectra of black hole X-ray novae at $E \lesssim 2$ keV.

2. Black Hole X-ray Novae and Neutron Star X-ray Novae

X-ray novae are characterized by episodic outbursts at X-ray, optical and radio frequencies, which are separated by long intervals (years to decades) of quiescence (Tanaka & Shibazaki 1996; van Paradijs & McClintock 1995). The outburst is caused by a sudden dramatic increase in the rate of mass accretion onto the compact primary. The X-ray flux rises on a time scale of the order of days, and the subsequent decline of the flux occurs on a time scale of weeks or months. The X-ray flux in outburst can be several million times the quiescent X-ray flux.

For a quiescent X-ray nova, the absorption-line velocities of the secondary star can be determined precisely. These velocity data *vs.* orbital phase determine the value of the mass function, $f(M)$, which gives an absolute lower limit on the mass of the compact primary. For 11 systems, $M_1 > f(M) \gtrsim 3M_\odot$. Assuming that general relativity applies, the maximum mass of a neutron star can be calculated to be about $2 - 3M_\odot$ (Cook et al. 1994; Kalogera & Baym 1996), so we can be almost certain that the compact primaries in these 11 systems are black holes. In addition the dynamical evidence is strong that two other systems (GRO 0422+32 and 4U1543-47) also contain black hole primaries. The masses and other dynamical data for these black-hole X-ray novae are discussed by Phil Charles in this volume.

A number of X-ray novae also contain neutron star primaries, as evidenced by the observation of type I X-ray bursts (Lewin, van Paradijs, & Taam 1995). A type I burst, which is a firm signature of a neutron star, is due to a thermonuclear flash in material that has been freshly accreted onto the star's surface. The phenomenology of these bursts has been closely studied since their discovery in 1975. The burst rise times are $\sim 1 - 10$ s and their decay times are ~ 10 s to minutes.

3. Evidence for Black Hole Event Horizons from Chandra

As discussed above, the best evidence for black holes comes from the dynamical studies of X-ray binaries that contain massive ($M_1 \gtrsim 3M_\odot$) compact stars. Unfortunately this evidence is not decisive; in particular, the limiting mass of a neutron star depends on the presumption that general relativity is the correct theory of strong gravity. If we hope to advance our position further, we must attempt to detect relativistic effects that are unique to compact objects. In this context, it would be especially important to show that one of the dynamical black hole candidates has an *event horizon*, which is the defining property of a black hole. Ramesh Narayan, Mike Garcia and I have pursued this goal for the past several years. Our approach has been to compare black hole X-ray novae and neutron star X-ray novae under similar conditions, to show that their luminosities differ greatly, and to interpret this luminosity difference in terms of advection-dominated accretion. In this section, I sketch this evidence for the detection of an event horizon. For a full account of this work, I refer you to a contemporaneous review by Narayan, Garcia & McClintock (2001; hereafter NGM01).

Table 1: QUIESCENT LUMINOSITIES OF NSXN AND BHXN

System	P_{orb} (hr)	$\log[L_{\text{min}}]$ (erg s $^{-1}$)
(1)	(2)	(3)
○ SAX J1808.4-3658	2.0	31.5
○ EXO 0748-676	3.82	34.1
○ 4U 2129+47	5.2	32.8
○ H1608-52	12	33.3
○ Cen X-4	15.1	32.4
○ Aql X-1	19	32.6
● GRO J0422+32	5.1	30.9 , < 31.6
● A0620-00	7.8	30.5 , 30.8
● GS 2000+25	8.3	30.4 , < 32.2
● GS1124-683	10.4	< 32.4
● H1705-250	12.5	< 33.0
● 4U 1543-47	27.0	< 31.5 , < 33.3
● GRO J1655-40	62.9	31.3 , 32.4
● V404 Cyg	155.3	33.7 , 33.1

NOTES — For references see Menou et al. (1999) and NGM01. New and/or *Chandra* Measurements are **in bold face**. (1) ○ indicates a neutron star primary and ● a black hole primary. (2) Orbital period. (3) Luminosity in quiescence in the 0.5-10 keV band.

3.1. Quiescent Luminosities of X-ray Novae

In order to fairly compare neutron star X-ray novae (NSXN) and black hole X-ray novae (BHXN), we must know their orbital periods, as this has a large influence on their mass transfer rates (Menou et al. 1999). In searching for differences between NSXN and BHXN, we have focused on X-ray observations of these systems in quiescence. We have examined the quiescent rather than the outburst state because we expect that the event horizon would be most apparent in quiescence. We are led to this expectation by the advection-dominated accretion flow (ADAF) model described below.

While there are now more than a dozen dynamically confirmed BHXN and a number of NSXN with known orbital periods, sensitive observations of the quiescent X-ray luminosity exist for only the subset of 8 BHXN and 6 NSXN listed in Table 1. We note that the tabulated luminosities assume an X-ray spectral shape and an estimate of the hydrogen column density to the source; however, the derived luminosities are weakly dependent on these assumptions (NGM01).

The key observational evidence for event horizons is summarized in Figure 1, where the Eddington-scaled quiescent luminosities of NSXN and BHXN are shown as a function of the binary orbital period P_{orb} . We scale the luminosity

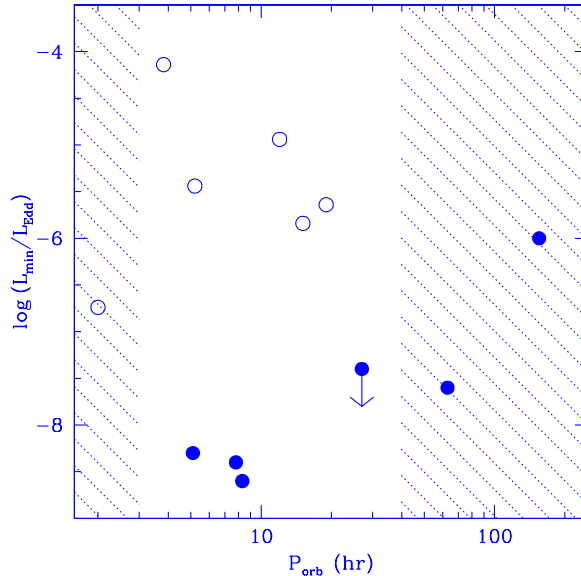


Figure 1. Quiescent luminosities of BHXN (filled circles) and NSXN (open circles) plotted against the binary orbital period. Only the lowest quiescent detections, or Chandra upper limits, are shown. The non-hatched region includes both BHXN and NSXN and allows both kinds of X-ray novae to be compared directly. The hatched region on the left has no BHXN and the region on the right has no NSXN; therefore these regions of the plot are less useful.

by the Eddington luminosity L_{Edd} under the reasonable assumption that the Eddington-scaled mass accretion rate is similar in quiescent BHXNs and NSXNs (NGM01). For the orbital period range in question, this assumption has been confirmed by model calculations (Menou et al. 1999).

Versions of Figure 1 were presented in earlier papers (e.g. Narayan, Garcia & McClintock 1997; Menou et al. 1999), and in each case we claimed that the data indicated that BHXN are substantially dimmer than NSXN in quiescence. The version shown here, which is taken from Garcia et al. (2001) and includes a number of sensitive BHXN measurements made with *Chandra*, greatly strengthens our earlier claims. We see that BHXN are dimmer than NSXN with comparable orbital periods by a factor of 100 or more (see the non-hatched region of the plot). Such a gross difference implies an important qualitative difference in the nature of the accretors in the two kinds of systems—e.g. the presence of an event horizon *versus* a surface, as discussed below.

At the shorter orbital periods, ($P_{\text{orb}} \lesssim 1$ day), the rate of mass transfer is rather low and is driven largely by gravitational radiation. Two BHXN are located at long orbital period in the cross-hatched region of Figure 1. For these systems, V404 Cyg and GRO 1655-40, nuclear evolution rather than gravitational radiation is expected to drive the mass transfer at a high rate, which is no longer uniquely determined by P_{orb} . Furthermore, there are no NSXN with

comparably long values of P_{orb} . For both reasons these particular BHXN are less useful for comparison. One NSXN with a very short orbital period, SAX J1808.4-3658, lies in the cross-hatched region on the left. It is also not useful since there is no comparison BHXN with a comparable period. This NSXN is also anomalous in being the only known millisecond X-ray pulsar (Wijnands et al. 1998).

3.2. Advection-Dominated Accretion and X-ray Binaries

Apart from the thin accretion disk, a second stable accretion flow solution is known, the so-called advection-dominated accretion flow (ADAF). The key feature of an ADAF (see NGM01, and references therein) is that the heat energy released by viscous dissipation is not radiated immediately, as in a thin disk, but is stored in the gas as thermal energy and advected with the flow—hence the name ADAF. Thus, as the gas falls into the deep potential well of the compact object, it becomes extraordinarily hot, $T_i \sim 10^{12}\text{K}/r$, where r is the radius in Schwarzschild units. At such temperatures, the gas bloats up around the compact object in a quasi-spherical cloud of low density gas.

The low density of an ADAF is a key property, since it reduces the number of particle-particle interactions, which thereby makes the plasma radiatively inefficient. The low density is also largely responsible for creating a two-temperature plasma, with the electrons being cooler than the ions, though still quite hot: $T_e > 10^9$ K. Heat energy from viscous dissipation is assumed to go primarily to the ions, which are inefficient radiators. Energy must be transferred from the ions to the electrons before it can be radiated, but that process is slow and the gas reaches the compact object first. Both because the energy is bottled up in the ions and because the radiative efficiency of the electrons is poor at low densities, the gas becomes advection-dominated.

Detailed calculations (Narayan & Yi 1995) show that the optically-thin two-temperature ADAF solution is allowed only for Eddington-scaled mass accretion rates $\dot{m} \equiv \dot{M}/\dot{M}_{\text{Edd}}$ less than a critical value $\dot{m}_{\text{crit}} \sim 0.01 - 0.1$. The X-ray spectra computed with the ADAF model match observations of BHXN in the *low hard* state quite well (Esin et al. 1997, 1998). Moreover, the prediction of a central hole in the thin disk that is filled with hot ADAF gas (Narayan, McClintock & Yi 1996; Narayan 1996; Esin et al. 1997) has been confirmed by recent observations of the BHXN XTE J1118+480 (McClintock et al. 2001; Esin et al. 2001; §4.2): the hole in the disk must have a radius $\gtrsim 55R_{\text{Schw}}$, rather than the $3R_{\text{Schw}}$ observed in the bright outburst state (see §4).

According to the above scenario, as the mass accretion rate decreases, the thin disk recedes to larger and larger radii and its luminosity falls rapidly. The emission from the ADAF also decreases substantially because the radiative efficiency decreases with decreasing \dot{m} (due to the lower density). The luminosity of the source thus falls steeply; roughly $L \sim \dot{m}^2$ (Narayan & Yi 1995). At sufficiently low \dot{m} , the luminosity corresponds to that observed in the quiescent state of X-ray novae, and in this state the ADAF zone is expected to be quite large ($\sim 10^3 - 10^4 R_{\text{Schw}}$ in models).

The ADAF model was first applied to the quiescent state of BHXN. Narayan, McClintock & Yi (1996) argued that the BHXN A0620-00 in quiescence has a spectrum that is inconsistent with a thin disk model, and showed that the spec-

trum can be explained with a model that has an ADAF at small radii and a thin disk at large radii. Narayan, Barret & McClintock (1997) modeled the relatively high signal-to-noise spectrum of the BHXN V404 Cyg and showed that the model again fits the observations quite well. Hameury et al. (1997) showed that the 6-day X-ray delay relative to the optical observed by Orosz et al. (1997) during the onset of an outburst of the BHXN GRO 1655-40 is best understood by invoking a hole in the thin disk, as postulated in the ADAF model.

3.3. The Event Horizon

The ADAF model plus the event horizon provide a straightforward explanation for the relative faintness of BHXN in quiescence. The reasoning is simple and based on the key feature of an ADAF: namely that most of the energy remains locked in the gas and is advected to the center. For quiescent X-ray novae, only a tiny fraction is radiated (less than 10^{-2} and as low as 10^{-4} in some models, compared to $\sim 10^{-1}$ for thin disk accretion). What happens to the bulk of the thermal energy, $\sim 0.1\dot{M}c^2$, when it arrives at the compact object?

If the accretor is a black hole, the advected energy disappears through the horizon as the gas falls in. But if the accretor is a neutron star, the gas will heat the surface of the star and radiate all its stored energy. Thus, for accretion via an ADAF the luminosity of a neutron star, or any object with a surface, will be significantly larger than an object with an event horizon (Narayan & Yi 1995; Narayan, Garcia & McClintock 1997; Garcia et al. 2001; NGM01). The data (Fig. 1) show clearly that quiescent BHXN are much dimmer than quiescent NSXN. Since we expect the two kinds of sources to have similar Eddington-scaled accretion rates (see above), we interpret the observations as the first clear evidence for the presence of event horizons in black hole candidates.

3.4. Further Developments in Theory and Modeling

The ADAF model discussed above is qualitatively consistent with the data in Figure 1; however, the situation is not as satisfactory on a quantitative level. The above model predicts that the difference in luminosity between BHXN and NSXN should be much larger than a factor of ~ 100 seen in the data. Menou et al. (1999) attribute this discrepancy to the NSXN, which they argue are anomalously dim because of the propeller action of a spinning magnetized neutron star (see NGM01).

ADAFs are convectively unstable (Narayan & Yi 1994, 1995). ADAFs with convection, which are called convection-dominated accretion flows, or CDAFs, are a new and important area of study (NGM01). Whether accretion proceeds via an ADAF or a CDAF, the mass that does reach the compact object will arrive at nearly the virial temperature with a great deal of thermal energy. Consequently, a BHXN will be significantly dimmer than an NSXN. Thus the interpretation of Fig. 1 as evidence for the event horizon is valid for either an ADAF or a CDAF. However, since the radiative efficiency of a CDAF is higher (for the same mass accretion rate), the difference in luminosity between BHXN and NSXN will be smaller than that estimated by Menou et al. (1999), who assumed an ADAF. In fact, Abramowicz & Igumenshchev (2001) have argued that the factor of 100 difference shown in Figure 1 between BHXN and NSXN is consistent with the CDAF model. Thus, the CDAF model provides a better

quantitative match between model predictions and observations of the luminosity, thereby strengthening the case for the detection of the event horizon. An important next step will be the computation of model spectra to compare with observations (e.g. Kong et al. 2001).

We have interpreted the data summarized in Figure 1 in terms of the ADAF model—i.e. we have assumed that X-ray novae are powered by accretion. However, several alternative models have been proposed to explain the difference in X-ray luminosity between BHXN and NSXN, most notably those by Bildsten and Rutledge (2000) and Brown, Bildsten & Rutledge (1998). For a critical discussion of these and other alternative models see NGM01.

4. X-ray Spectra of BHXN at Energies Below ~ 2 keV

The quest to detect a black hole event horizon may seem somewhat inflated as a topic, so I have picked something quite modest to end with. Namely, the spectra of accreting black holes at energies below ~ 2 keV. The flavor of this topic is similar to many other topics that Jan and I discussed over the years.

4.1. The High/Soft State

For BHXN in the *high/soft* state, the spectrum can be very well modeled by a multi-temperature disk blackbody (Mitsuda et al. 1984; Makashima et al. 1986). In this state, there is good evidence that the accretion disk extends inward to the minimum stable circular orbit at $R_{\text{ms}} = 3R_{\text{Schw}}$ (Tanaka & Shibazaki 1996; Sobczak et al. 1999). The low energy spectrum of a BHXN in the *high/soft* state may approximate the model disk spectrum fairly well; however, because of interstellar absorption no sensitive observations have been made at low energies ($E < 1$ keV) that confirm this conjecture.

4.2. The Low/Hard State of XTE J1118+480

For a BHXN in the *low/hard* state, it has been believed for some time that the inner edge of the accretion disk is located far outside the minimum stable orbit, which is located at $3R_{\text{Schw}}$. The presence of a large hole in the inner disk was predicted by ADAF theory (Narayan, McClintock & Yi 1996; Narayan 1996; Esin, McClintock & Narayan 1997), and further support for this picture was provided subsequently by Compton reflection models that were constructed for several sources (e.g. Gierlinski et al. 1997; Zycki, Done & Smith 1998).

In March of last year, XTE J1118+480 erupted. The source's high-latitude ($b = 62^\circ$) and extraordinarily low column depth, $N_{\text{H}} \approx 1 \times 10^{21} \text{ cm}^{-2}$, gave us our first penetrating look at the low-energy spectrum of a BHXN in the *low/hard* state. Two major multiwavelength studies were conducted, one by Hynes et al. (2000) and the other by McClintock et al. (2001). Both studies feature near-simultaneous radio, UKIRT IR, HST/STIS, EUVE and RXTE data. In addition, the latter study also includes simultaneous Chandra LETG/ACIS grating data that covers the energy range 0.24–6 keV.

For a global view of the spectrum, which consists of two components, see Figure 4 in McClintock et al. (2001). The quasi power-law spectral component, which was observed from 0.4–160 keV, was modeled successfully as an ADAF

(Esin et al. 2001). Below ~ 0.4 keV, the spectrum is dominated by a ≈ 24 eV thermal component that is attributed to an accretion disk with a large inner disk radius: $\gtrsim 55R_{\text{Schw}}$ (Esin et al. 2001), which is about 20 times larger than the radius of the minimum stable orbit ($3R_{\text{Schw}}$). In conclusion, the low energy spectrum of the *low/hard* state has been closely observed.

4.3. The Very High State of XTE J1550-564

Unfortunately, we have yet to observe a high latitude BHXN in the *very high* state. Nevertheless, I will argue that the extensive spectral and timing results obtained for XTE J1550-564 give us some insight into the *very high* state spectrum of this source below ~ 2 keV, despite its large column depth, ($N_{\text{H}} \sim 10^{22}$ cm $^{-2}$) (Sobczak et al. 2000; Tomsick et al. 2001). A total of 209 pointed observations of XTE J1550-564 were made during its 250-day outburst in 1998-99. The spectra are generally well-fitted by a model comprised of disk blackbody plus power-law components as discussed in detail by Sobczak et al. (2000). Low-frequency QPOs were detected in 72 of the 209 observations and fruitfully divided into three types based on their phase lags and other properties by Remillard et al. (2001). Here we consider only the subset of 46 observations that yielded “type C” low-frequency QPOs.

In the context of the disk blackbody model, Remillard et al. (2001) examined the correlation between the central frequency of the type C QPOs and the flux from the accretion disk. Because the temperature of the inner disk of XTE J1550-564 is cool, ($kT_{\text{in}} \approx 0.6$ keV), we faced a serious difficulty in defining the accretion disk flux, since a large fraction of this soft flux is cut off by the ISM and the PCA response and could not be observed (see Fig. 2). We therefore considered two measures of the disk flux: (1) The observed 2-20 keV flux and (2) the bolometric flux, $F_{\text{bol}} \propto R_{\text{in}}^2 \times T_{\text{in}}^4$, where R_{in} is the inner disk radius (Mitsuda et al. 1984; Makashima et al. 1986). It was not obvious to us which of these measures of the disk flux one should correlate against the QPO frequency, so we prepared the two correlation plots shown in Figure 3 (Remillard et al. 2001; see their Fig. 5 for additional correlations between QPO parameters and spectral parameters).

The excellent correlation shown in Figure 3a between an oscillation frequency and the observed 2-20 keV accretion disk flux strikes me as extraordinary. Especially when one considers the enormous amplitudes of these oscillations, which range from 5-15% (rms; see Fig. 5 in Remillard et al. 2001). How are such powerful oscillations coupled so effectively to the disk flux?

The correlation of frequency with bolometric flux in Figure 3b is shabby at the higher frequencies. This result may be caused by sizable uncertainties in both T_{in} and R_{in} combined with the large extrapolation required to compute the bolometric flux. On the other hand, the model’s failure may be caused by the failure of the disk blackbody model itself, which brings me to my last point. In Figure 4, I show a typical *very high* state spectrum of XTE J1550-564. As shown, in this state the accretion disk component is a tiny fraction of the total flux, which makes the tight correlation shown in Figure 3a all the more remarkable. All along, I have been referring to this soft component as thermal emission from an accretion disk (cf. Sobczak et al. 2000). However, at this symposium Fred Lamb pointed out to me that this soft flux is more likely

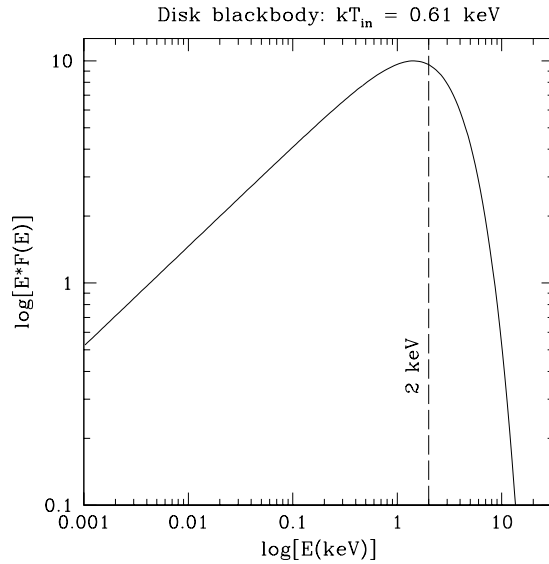


Figure 2. A disk blackbody model spectrum generated using XSPEC (diskbb) for the average disk temperature determined by Sobczak et al. (2000) for the 46 observations that exhibited type C QPOs (Remillard et al. 2001). Note that the quantity on the y-axis is ($Energy \times Energy\ flux$). The dashed vertical line indicates the approximate low-energy cutoff of the RXTE PCA and the ISM

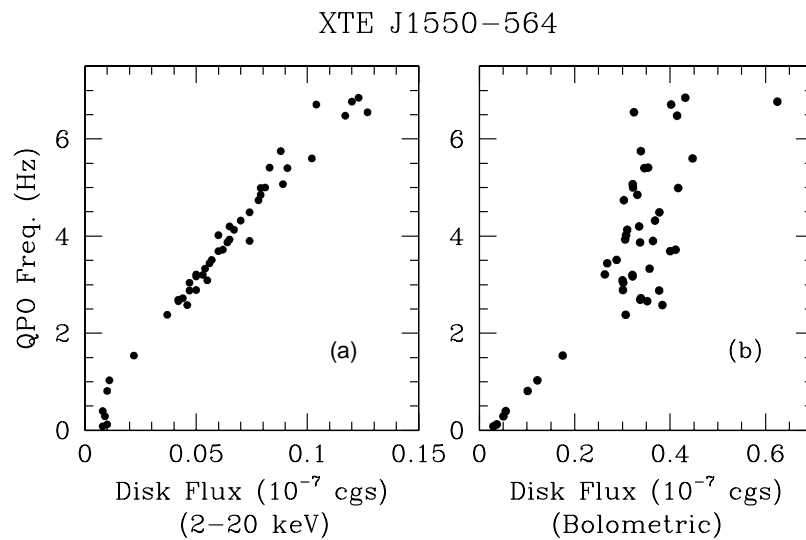


Figure 3. QPO central frequency for Type C QPOs *vs.* the disk flux in units of $10^{-7} \text{ ergs cm}^{-2} \text{ s}^{-1}$. (a) The unabsorbed flux measured over the observed 2–20 keV band. (b) The bolometric disk flux.

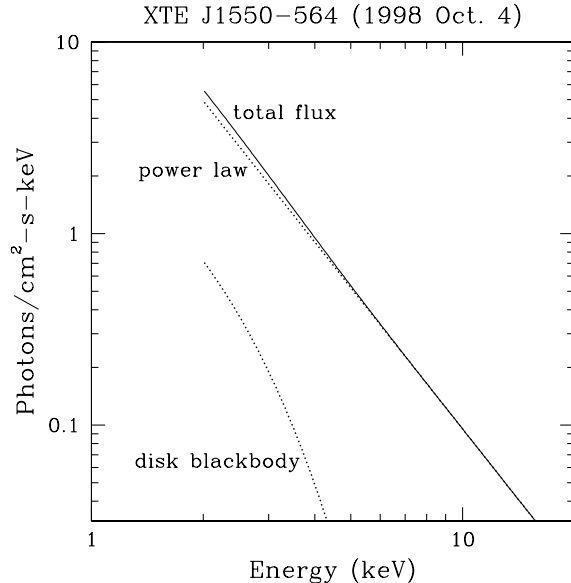


Figure 4. The solid line shows a typical PCA *very high* state spectrum of XTE J1550-564 obtained when type C QPOs were present (observation no. 36; Sobczak et al. 2000). The dashed lines show the disk blackbody ($kT_{\text{in}} = 0.64$ keV) and power-law (photon index = 2.45) components of emission. The statistical uncertainties in the spectral parameters are very small (see Table 2 in Sobczak et al. 2000).

a Comptonized component of emission, which one might expect to find in the presence of the dominant power-law component (Fig. 4).

In conclusion, in an effort to be as objective as possible, I now refer to this soft spectral component in the *very high* state as the “non-power-law” component—i.e. the residual flux that remains after fitting a pure power-law to the data. The relative contribution of this non-power-law component increases with decreasing energy, reaching $\approx 15\%$ at 2 keV (Fig. 4). Clearly it will be important to capitalize on any rare future opportunities that may arise to observe the low energy spectrum and other properties of this soft emission component, which is coupled so strongly to the powerful low-frequency QPOs.

Acknowledgment: §3 on black-hole event horizons draws heavily on a major review by Narayan, Garcia and McClintock (2001; NGM01). I am grateful to Ramesh Narayan and Mike Garcia for permission to make use of this material. This work was partially supported by NASA grants NAG5-10813 and GO0-1105A.

References

- Abramowicz, M.A., & Igumenshchev, I.V. 2001, ApJ, 554, L53
 Bildsten, L., & Rutledge, R.E. 2000, ApJ, 541, 908
 Brown, E.F., Bildsten, L., & Rutledge, R.E. 1998, ApJ, 504, L95

- Cook, G.B., Shapiro, S.L., & Teukolsky, S.A. 1994, ApJ, 424, 823
- Esin, A.A., McClintock, J.E., Drake, J.J., Garcia, M.R., Haswell, C.A., Hynes, R.I., & Munro, M.P. 2001, ApJ, 555, 483
- Esin, A.A., McClintock, J.E., & Narayan, R. 1997, ApJ, 489, 865; 500, 523
- Esin, A.A., Narayan, R., Cui, W., Grove, J., & Zhang, S. 1998, ApJ, 505, 854
- Garcia, M.R., McClintock, J.E., Narayan, R., Callanan, P., Barret, D., & Murray, S.S. 2001, ApJ, 553, L47
- Gierlinski, M., Zdziarski, A.A., Done, C., et al. 1997, MNRAS, 288, 958
- Hameury, J., Lasota, J., McClintock, J., & Narayan, R. 1997, ApJ, 489, 234
- Hynes, R.I., Mauche, C.W., Haswell, C.A., Shrader, C.R., Cui, W., & Chaty, S. 2000, ApJ, 539, 37
- Kalogera, V., & Baym, G. 1996, ApJ, 470, L61
- Kong, A.K.H., et al. 2001 in preparation
- Lewin, W.H.G., van Paradijs, J., & Taam, R.E., in X-ray Binaries, eds. W. Lewin, J. van Paradijs, & E. van den Heuvel (CUP: Cambridge) p175
- Makashima, K., Maejima, Y., Mitsuda, K., et al. 1986, ApJ, 308, 635
- Menou, K., Esin, A.A., Narayan, R., Garcia, M.R., Lasota, J.-P., & McClintock, J.E. 1999, ApJ, 520, 276
- McClintock, J.E., Haswell, C.A., Garcia, M.R., Drake, J.J., Hynes, R.I., et al. 2001, ApJ, 555, 477
- Mitsuda, K., Inoue, H., Koyama, K., et al. 1984, PASJ, 36, 741
- Narayan, R. 1996, ApJ, 462, 136
- Narayan, R., Barret, D., & McClintock, J.E. 1997, ApJ, 482, 448
- Narayan, R., Garcia, M.R., & McClintock, J.E. 1997, ApJ, 478, L79
- Narayan, R., Garcia, M.R., & McClintock, J.E. 2001, to appear in Proc. IX Marcel Grossmann Meeting, eds. V. Gurzadyan, R. Jantzen and R. Ruffini (Singapore: World Scientific) (astro-ph/0107387) [NGM01]
- Narayan, R., McClintock, J.E., & Yi, I. 1996, ApJ, 457, 821
- Narayan, R., & Yi, I. 1994, ApJ, 428, L13
- Narayan, R., & Yi, I. 1995, ApJ, 452, 710
- Orosz, J., Remillard, R., Bailyn, C., & McClintock, J. 1997, ApJ, 478, L83
- Remillard, R.A., Sobczak, G.J., Munro, M.P., & McClintock, J.E. 2001, ApJ, in press (astro-ph/0105508)
- Sobczak, G.S., McClintock, J.E., Remillard, R.A., Bailyn, C.D., & Orosz, J.A. 1999, ApJ, 520, 776
- Sobczak, G.J., McClintock, J.E., Remillard, R.A., et al. 2000, ApJ, 544, 993
- Tanaka, Y., & Shibazaki, N. 1996, ARAA, 34, 607
- Tomsick, J.A., Corbel, S., & Kaaret, P. 2001, ApJ, submitted (astro-ph/0105394)
- van Paradijs, J., & McClintock, J.E. 1995, in X-ray Binaries, eds. W. Lewin, J. van Paradijs, & E. van den Heuvel (CUP: Cambridge) p58
- Wijnands, R., & van der Klis, M. 1998, Nature, 394, 344
- Zycki, P.T., Done, C. & Smith, D.A. 1998, ApJ, 496, L25